Study on Structural and Hydrodynamics of Autonomous Underwater Gliders

by

Nadhira Binti Mohd Khairuddin

13763

Dissertation submitted in partial fulfilment of
the requirements for the
Bachelor of Engineering (Hons)
(Mechanical)

MAY 2014

Universiti Teknologi PETRONAS
Bandar Seri Iskandar
31750 Tronoh
Perak Darul Ridzuan

CERTIFICATION OF APPROVAL

STUDY ON STRUCTURAL AND HYDRODYNAMICS OF AUTONOMOUS UNDERWATER GLIDERS

by

NadhiraBintiMohdKhairuddin

13761

A project dissertation submitted to the

Mechanical Engineering Programme

UniversitiTeknologi PETRONAS

In partial fulfilment of the requirement for the

BACHELOR OF ENGINEERING (Hons)

(MECHANICAL)

Approved by,

_____

(Dr. Mark Ovinis)

UNIVERSITI TEKNOLOGI PETRONAS

TRONOH, PERAK

May 2014

CERTIFICATION OF ORIGINALITY

This is to certify that I am responsible for the work submitted in this project, that the original work is my own except as specified in the references and acknowledgements, and that the original work contained herein have not been undertaken or done by unspecified sources or persons.

NADHIRA BINTI MOHD KHAIRUDDIN

ACKNOWLEDGEMENT

Special thanks to my supervisor Dr. Mark Ovinis for his dedication helps to spend his precious time to teach, and guide me despite he has many other obligations. My gratitude towards my post graduate student, Mr Yasser for sharing his expertise and teach me about statistical knowledge and always keeping his door open. Many thanks to my family back home for their sacrifices coupled with their continuous encouragement and support and heading me towards the stars. Special thanks to all the friends that help me completing this project, patiently teach me the technical basic of the project and for together brainstorming in order to encounter problem faced. Each and every helps of them means the world to me.

ABSTRACT

Underwater gliders are autonomous underwater vehicles that use buoyancy to convert horizontal to vertical displacement to propel underwater. The most famous and common AUGs in the market are Slocum, Seaglider, Spray, and LiberdadeXray. All these gliders serve at different operating depth and payload. However, external forces and hydrodynamic forces are important to define the operational capacity of an AUG. Experimentally, it is expensive and difficult to determine the behaviour of structural and hydrodynamic forces. Therefore simulation is used to optimize the structural and hydrodynamics of the AUGs. There are two types of analysis proposed to compare both Slocum and Seaglider which are structural FEA and hydrodynamic CFD analysis. For structural FEA analysis, CATIA Dessault software is used meanwhile ANSYS FLUENT is used to analysis hydrodynamic performance of these AUGs. For the structural analysis, FEA modelling has been used to test the Von Mises stress and buckling of three types of materials on the AUGs hull body. On the other hand, hydrodynamic performance of the AUGs are tested to interpret the coefficient of lift, coefficient of drag and lift to drag ratio generated on Slocum and Seaglider at different angle of attacks ($-15° - +15°$). For this project, these findings are to be compared between the chosen gliders based on structural and hydrodynamic performance. From structural perspective, it is found that Seaglider has better hull body performance compared to Slocum because Seaglider is designed at thicker hull thickness and higher buckling resistance compare to Slocum. Based on hydrodynamic performance, Seaglider also has higher performance than Slocum because Seaglider produced less drag and higher lifted when simulated at different angles of attacks. This is because an AUG shape greatly influences its hydrodynamic performance. Seaglider has shape more closely to NACA airfoil design which performs to have less drag and higher lift.

TABLE OF CONTENT

LIST OF TABLES

LIST OF FIGURES

LIST OF ABBREVIATIONS

AUG **Autonomous Underwater Glider**

CFD **Computational Fluid Dynamic**

FEA **Finite Element Analysis**

AoA **Angle of Attack**

CHAPTER 1
INTRODUCTION

1.0 INTRODUCTION

1.1 Background of study

Autonomous underwater gliders (AUGs) are a type of underwater vehicles that do not use convention propulsion method. These vehicles glide and manoeuvre either in shallow or deepwater ocean at low speed by changing buoyancy for vertical movement and wings to glide horizontally. In this era, AUGs are rapidly developed mainly in oceanography and military and defence area. This development does not only essentially economy but it broadens the development in marine technology especially for deepwater purpose.

The need for technology to collect oceanic samples by remote control without the cost of ships was recognized by Henry Stommel in the early days of World Ocean Circulation Experiment (WOCE) [1]. This perspective has driven him to analyse a method that would provide subsurface data on a scale and at a frequency that matched what remote sensing by satellite provided for the sea surface [1]. Henry Stommel published an article concerning technical specifications for the gliders he described and his concept are now being adopted in current AUGs developments.

However, in 1988, Doug Web, a research engineer proposed an idea for thermal powered glider in line with Stommel's vision on AUGs. The newly designed AUG, Slocum, was named after Joshua Slocum who was the first single-handed global circumnavigation man who sailed with sailboat. Furthermore, the research and development of AUGs are rapidly developed throughout the years and many commercial gliders are produced with the same purpose such as Spray, Seaglider, Bluefin robotics, Liberdade Xray and Zray. The design philosophy of AUGs are based on profiling floats or commercially known as Argo. Argo is a global array which floats and it functions to measure the temperature and salinity of the ocean.

1.2 Problem Statement

External forces and hydrodynamic forces are important to define the operational capacity of an AUG. Experimentally, it is expensive and difficult to determine the behaviour of structural and hydrodynamic forces. Therefore simulation is used to optimize the structural and hydrodynamics of the AUGs.

1.3 Objective

- To evaluate design of Slocum and Seaglider at maximum operating pressure with different materials.
- To evaluate the hydrodynamic performance of Slocum and Seaglider at different angles of attack.

1.4 Scope of Study

This study is focus on the comparative design of existing AUGs by using CATIA and SolidWorks modelling software and the finite volume based CFD software FLUENT 6.1.3 will be used for 3D simulations, by exploiting the k- epsilon turbulence model.

CHAPTER 2

LITERATURE REVIEW

2.0 LITERATURE REVIEW

2.1 Comparison of Existing Gliders Design

Currently, five significant gliders designs are in used commercially which are Slocum [7], Spray [4], and Seaglider [5], Liberdade Xray and Bluefin robotics. Slocum is designed to glide in shallow water operation and its battery is designed to commission with low hydrodynamic drag in aluminum hull body. A large single stroke pump installed in the hull body pushes out the amount of water entering and leaving the hull during shallow pressure operation. Thus, the pump is designated to function more efficiently in shallow water than deepwater activities.

Alternatively, Spray is designed for endurance, long range and deepwater operations. The hydrodynamic drag of Spray is 50% higher than Slocum because it employs better hull shape. However, Spray glider operates on high pressure wobble plate reciprocating pump and external bladders which is hydraulically configured similar to ALACE floats [6]. Meanwhile, battery powered sea glider is optimized to operate under one-year duration and ocean basins ranges. By having a maximum diameter of 70% of the body length from nose with a low-drag hydrodynamic designed body, laminar boundary layer is sustained.

Meanwhile, Slocum glider is well known on its versatility, maneuverability and it operates by alkaline batteries. This electric glider can be deployed for a period of 15 to 30 days at a 600- to 1500-km range. Its flexible payload allows it to carry customized sensors. The coastal glider can be operated to depths of 4–200 meters and the 1-km glider to 1000 meters.

The Bluefin-21 has an extraordinary design which is able to carry multiple sensors and payloads at once. This AUG has high energy capacity that can perform long duration operations even at the greatest depths. The Bluefin-21 has immense capability but is also flexible enough to operate from various ships of opportunity worldwide.

Liberdade Xray glider has the largest design (6.1 metres wing span) among all gliders which has an advantage in terms of hydrodynamic performance and this design enables to carry large payload. Moreover, this AUG was designed offers easy deployment capability and at the same time it can carry large payload which is currently better than the existing glider.

Attribute	Slocum	Spray	Seaglider	Liberdade Xray	Bluefin21
					
Hull design	1.5 m length, 21.3 cm diameter	2m length, 20 cm diameter	1.8m length, 30 cm diameter	6.1 m wing span	4.9 m length, 53 cm diameter
Mass	52 kg	51 kg	52 kg	700 kg	750 kg
Horizontal speed	0.4 m/s	0.45 m/s	0.45 m/s	-	-
Max. depth	200 m	1500 m	1000m	300m	4500 m
Payload	5 kg	3.5 kg	4 kg	6 kg	7.3 kg

Table 2.1: Design comparison of the commercial existing gliders

Based from the above comparison, Bluefin21 has the longest operation depth up to 4500 metres and followed by Spray glider which has a depth range up to 1500 metres. However, with a maximum depth range of 1500 metres, Spray glider does not carry large payload as compared with Bluefin21. On the other hand, Slocum and Liberdade Xray gliders are only designed for shallow water operations because their depth ranges are less than 1200 metres. However, in terms of payload capability, these shallow water based gliders are able to carry larger payloads as compared to the deepwater gliders such as Spray and Seaglider.

2.2 Hydrodynamic Performance

The upward and downward movements of AUGs are based from the buoyancy principle by which the AUGs maneuvered vertically and wings to glide horizontally. Figure 2.1 shows a common dive profile used to describe AUG gliding operation. One of the major factors which contribute to the motion of the AUGs is hydrodynamic forces and moments of the body and wings. Lift and drag are both important factors to determine AUGs capabilities and horizontal translation in order to achieve forward movement. Furthermore, drag and lift forces calculation is elaborated in Results and Discussion section. On the other hand, there are a number of other contributing factors on the AUG hydrodynamic performance which are the lift force on the wings, drag force on the body, drag force on the wings and drag force on the tail which are shown in Figure 2.1 below.

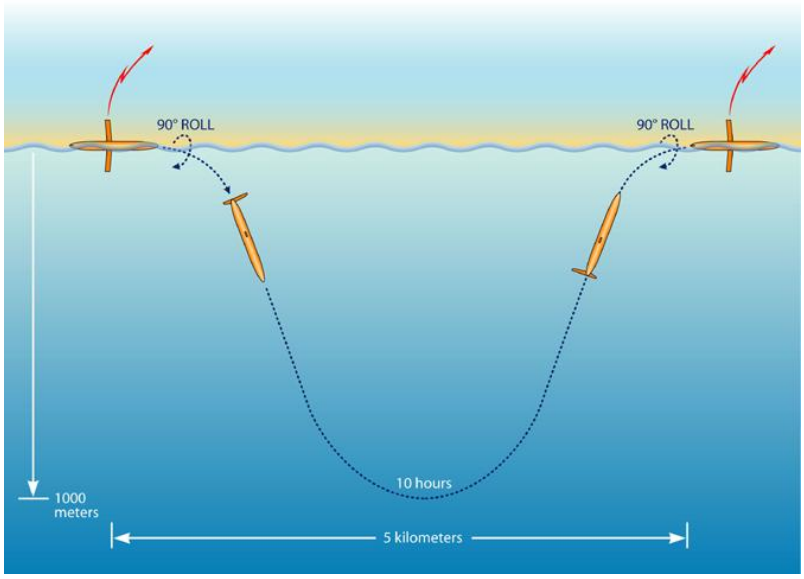

Figure 2.1: Common dive profile to describe an AUG operation

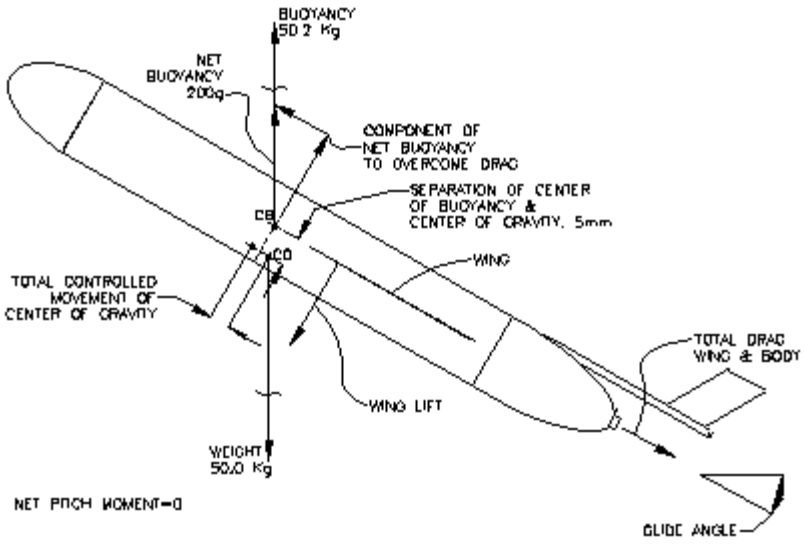

Figure 2.2: Forces acted on AUGs

The AUGs glide angle can be determined by summing of the lift and drag forces at a specific velocity. As shown in Equation 2.1 and in Figure 2.2, glide angle,θ, is the angle between the velocity vector and the horizontal line. Table 2.2 below shows a list of abbreviation of each force shown in Figure 2.2

Table 2.2: List of abbreviation of each force shown in Figure 2

Forces	Symbol
Coefficient of drag wing	C_{DW}
Coefficient of drag body	C_{DB}
Coefficient of drag tail	C_{DT}
Coefficient of lift of wing	C_{LW}
Wing area	A_w
Tail area	A_T
Fairing cross sectional area	A_B

These variables are discussed in Chapter 4.

$$\tan\theta = \frac{A_W C_{DW} + A_B C_{DB} + A_T C_{DT}}{A_W C_{LW}} \quad (2.1)$$

2.3 Pitch Control

Pitch, and consequently dive angle is generally regulated by displacing AUG internal mass force. Typically, internal mass consist of batteries which is placed on a portable sledge. On the other hand, some AUG's main pitching moment is needed in between upward and downward drift which is achievable by positioning the bladder or movable ballast at the nose of the AUG. Moreover, by changing the position of the centre of buoyancy and the centre of gravity generate a moment that casts AUG. When the center of gravity (CG) is ahead of center of buoyancy (CB), it gives a negative angle of attack and by which the AUG's body and wings produce longitudinal hydrodynamic component to propel the underwater vehicle as it manoeuvres. However, the angle of attack will be positive when CG is beyond CB when the AUG ascends. Fine control of the pitch angle is then achieved by shifting the internal mass [2].

CHAPTER 3
METHODOLOGY

3.0 METHODOLOGY

Design methodology of AUG is discussed in this chapter to identify overall generalization stages at which a disseminated process can be assessed. The main objective of identifying these overall generalization stages is to make comparative structural design of existing AUGs with different type of materials and to compare AUGs hydrodynamic behavior and dive profiling. There are two main stages under this project which are structural analysis and hydrodynamic analysis. In order to carry out this project, the process required is proposed as shown in the design methodology below.

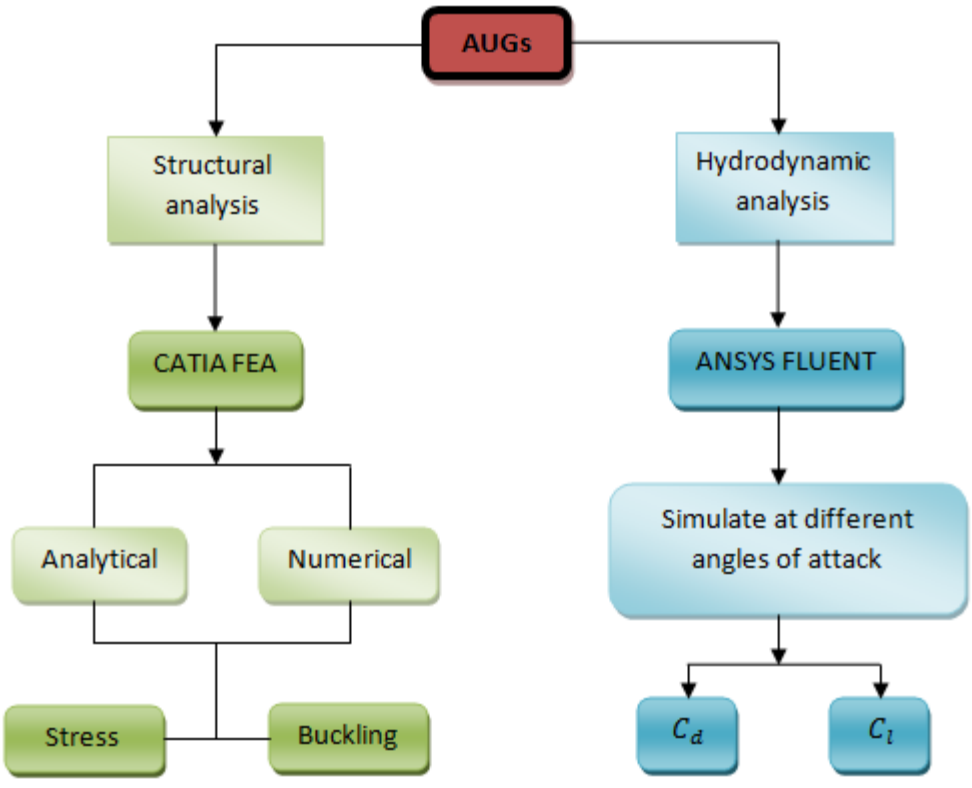

Figure 3.1: Methodology flow of the project

3.1 Tools and Software Required

Tools and Software required are as follows:

1. CATIA Dassault Systemes
2. SolidWorks
3. ANSYS Fluent 6.1.3

3.2 Gantt -Chart and Key Milestone

Project Work	Week																											
	1	2	3	4	5	6	7	8	9	10	11	12	13	14	15	16	17	18	19	20	21	22	23	24	25	26	27	28
Title Selection																												
Feasibility study																												
Develop project proposal						**1**																						
Approve project proposal																												
Identify governing equations																												
Specify detail requirements																												
Solid modelling														**14**														
Develop hydrodynamic simulation																												
Develop prototype																												
Approve prototype																												
FEA design analysis																					**3**							
Debugging and Improvement																									**4**	**5**		
Project Demonstration and Conclusion																										**6**	**7**	

Key Milestone

1. Submission of extended proposal
2. Submission of interim report
3. Submission of progress report
4. Submission of final report
5. Submission of dissertation
6. Submission of technical paper
7. Viva presentation

CHAPTER 4

RESULTS AND DISCUSSIONS

4.0 RESULTS AND DISCUSSIONS

In this chapter, the findings are divided into 2 main parts which are;

1. Structural analysis
2. Hydrodynamic analysis

The analysis made is resulted from the current AUGs which are Slocum, Seaglider and Liberdade Xray. The two main findings are divided into few sub-parts which are to be discussed further along the discussions.

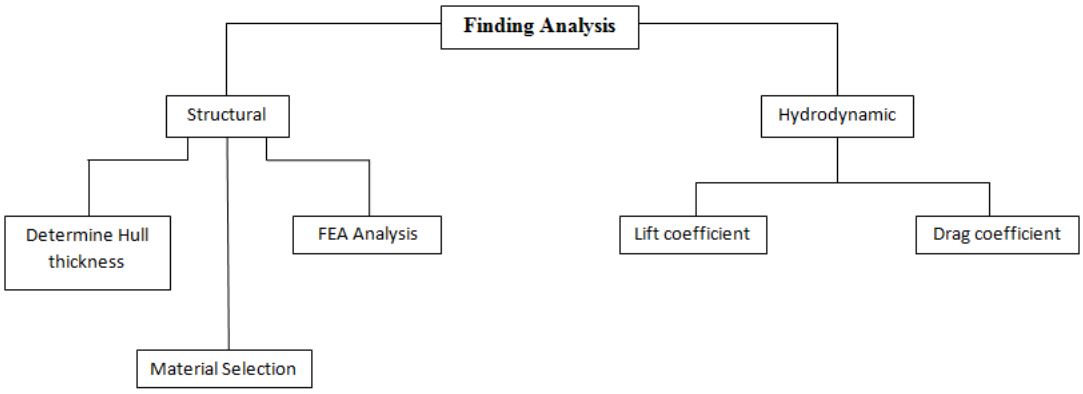

4.1.1 Structural analysis

Different AUGs operate at different water depth and has different maximum operating pressure. In order to design a hull body which operates at optimum depth and carry large payload, the hull is designed to have less mass and larger containing space for devices storage.

Table 4.1: Maximum working pressure tested at maximum depth on each AUG model

Model	Operating Depth (ft)	Maximum Working Pressure (Psi)	Mpa
Slocum	656	299	2.03
Seaglider	3280	1435	9.76

Therefore, hull thickness of each AUG is calculated with comparison among three different kinds of materials – aluminium alloy, titanium alloy and stainless steel which are commonly used for hull fabrication of underwater vehicles. Moreover, these calculated results are then being compared to FEA analysis which is made by using CATIA Dessaults. The wall thickness of the hull is determined by Roark's Equation which is as follows;

$$\delta_y \geq \frac{P_{max} D_i}{2[\sigma]\varphi_s - P_{max}} + C \qquad (4.1)$$

Where;

P_{max}	Maximum Working Pressure
D_i	Inner Diameter of Hull
σ	Permissible stress
C	Additional Value of Wall Thickness
φ_s	Weld Joint Efficiency
δ_y	Wall Thickness of Strength Check

Table 4.2: Calculated results of wall thickness of the hull body of AUGS with different types of materials

			Aluminum Alloy		Titanium Alloy		Stainless Steel	
Measuring Parameters		Units	Slocum	Seaglider	Slocum	Seaglider	Slocum	Seaglider
Maximum Working Pressure	P_{max}	MPa	2.03	9.76	2.03	9.76	2.03	9.76
Inner Diameter of Hull	D_i	mm	180	250	180	250	180	250
Permissible stress	σ	MPa	69000	69000	115000	115000	190000	190000
Additional Value of Wall Thickness	C	mm	0.01	0.01	0.01	0.01	0.01	0.01
Weld Joint Efficiency	φ_s	-	1	1	1	1	1	1
Wall Thickness of Strength Check	δ_y	mm	0.013	0.028	0.012	0.021	0.01096	0.01547

Table 4.2 gives the characteristic and wall thickness calculation results of the three types of materials. However, Slocum and Seaglider's hulls are characterized as thin walled cylindrical body which needs wall thickness buckling check. For this analysis, circumferential and axial buckling checked is taken into account. Again, the buckling wall thickness and permissible critical stress of axial buckling are calculated by using Roark's equation which are as follow;

Buckling wall thickness equation;

$$\delta_{bc} \geq D_o\left(\frac{m_c P_{max} L}{2.59 E D_o}\right)^{0.4} \qquad (4.2)$$

D_o	Outer Diameter
m_c	Safety Factor
P_{max}	Maximum operating pressure
L	Length of Hull
E	Elastic Modulus of Material

Table 4.3: Calculated wall thickness of circumference of different type of AUGs with different type of materials

			Aluminium Alloy		Titanium Alloy		Stainless Steel	
Measuring Parameters		Units	Slocum	Seaglider	Slocum	Seaglider	Slocum	Seaglider
Outer Diameter	Do	mm	213	300	213	300	213	300
Safety Factor	m_c	-	2	2	2	2	2	2
Maximum operating pressure	P_{max}	MPa	2.03	9.76	2.03	9.76	2.03	9.76
Length of Hull	L	mm	1500	1800	1500	1800	1500	1800
Elastic Modulus of Material	E	MPa	69000	69000	115000	115000	190000	190000
Wall Thickness of circumferences	δ_{bc}	mm	6.46	15.99	5.26	13.03	4.31	10.66

Permissible critical stress of axial buckling equation;

$$[\sigma_{cr}] = \frac{P_{max} R}{\delta_{bc}} \qquad (4.3)$$

Where;

P_{max} Maximum operating pressure

R Radius of Intermediate Surface of Hull

∂_{bc} Wall thickness of circumference

σ_{cr} Permissible Critical Stress of Axial Buckling

Table 4.4: Calculated Axial stress of different type of AUGs with different type of materials

		Aluminium Alloy		Titanium Alloy		Stainless Steel	
Measuring Parameters	Units	Slocum	Seaglider	Slocum	Seaglider	Slocum	Seaglider
Maximum operating pressure	MPa	2.03	9.76	2.03	9.76	2.03	9.76
Radius of Intermediate Surface of Hull	mm	106.5	150	106.5	150	106.5	150
Wall Thickness of Hull	mm	12.10	15.00	9.86	12.23	8.07	10.00
Axial stress	MPa	17.87	97.60	21.92	119.75	26.79	146.39

4.1.2 FEA Analysis

A finite element analysis was carried out by using CATIA Dessaults software to verify the calculations. However this method was used due to certain reasons. The major aim of this analysis is to provide verification of the calculated results obtained by using theoretical methods and formula. Besides that, FEA analysis is used to investigate the overall buckling behaviour of the body geometries. There are two results produced from each model of AUG with different type of materials used which are aluminium alloy, titanium alloy and stainless steel. The two results obtained are Von Misses Stress analysis and wall thickness of strength check analysis for the pressure hull structure.

For this analysis, the pressures applied to the hull structure of AUGs are different because Slocum and Seaglider operate at different pressures which are 2.03 MPa, and 9.76 MPa respectively.

SLOCUM

i. Aluminium Alloy

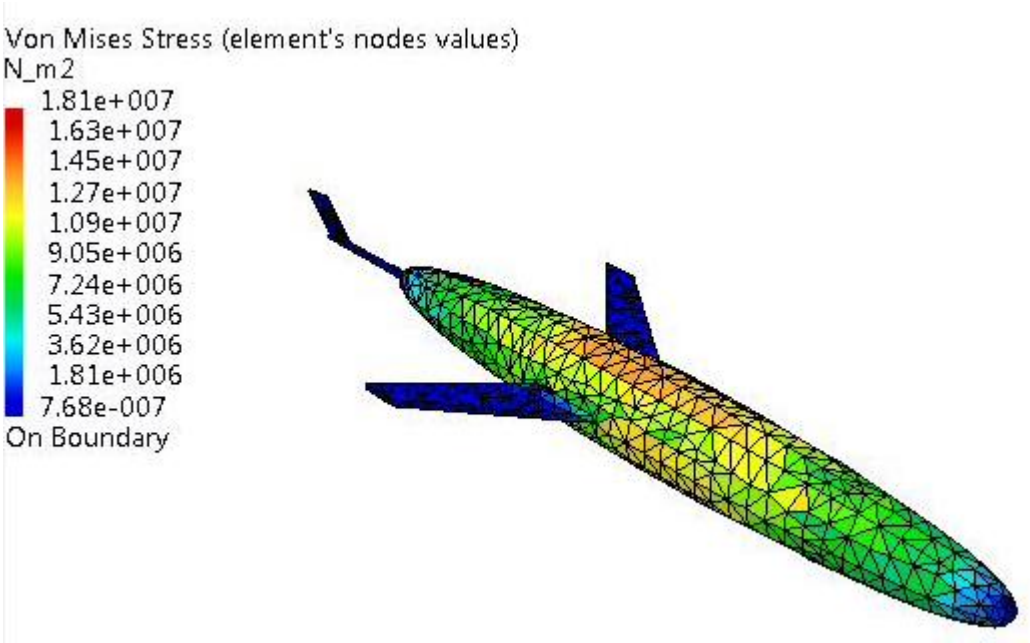

Figure 4.1: Von Mises stress on Slocum with Aluminium alloy body

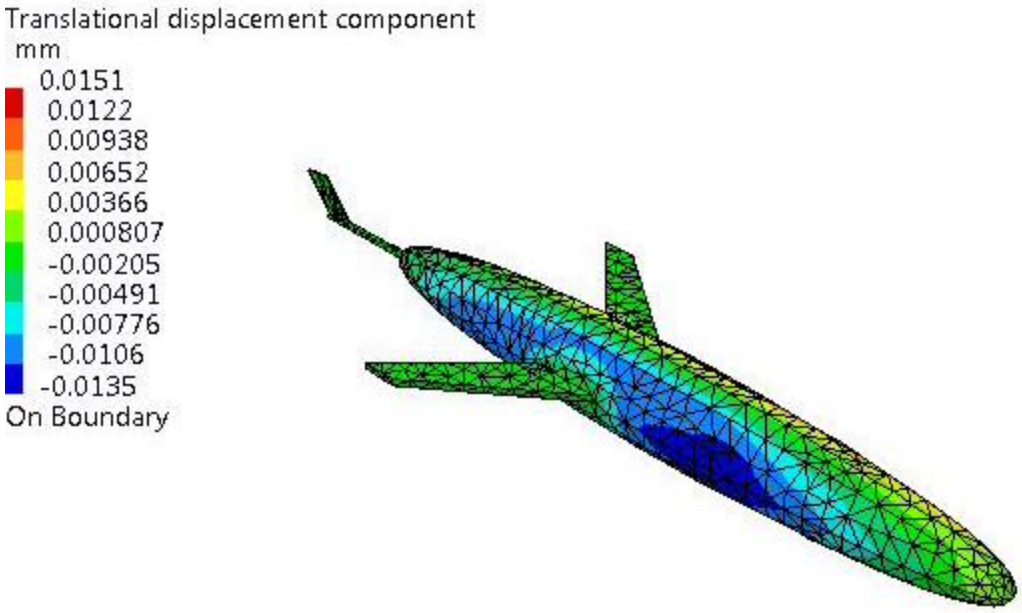

Figure 4.2: Displacement vector on Slocum with Aluminium alloy body

Figure 4.1 and Figure 4.2 show Von Mises stress and displacement vector generated on Slocum by numerical method on aluminium alloy body respectively. From the analysis above, we can interpret that the most highly distorted element is located at the middle of the glider body which is at 18.1 MPa. On the other hand, the result of translational displacement is highest at the tip and tail of the glider. It is interpreted that the result from the displacement indicated the buckling effect of the glider. Based from the simulation made, both Von Mises stress and translational displacement are within the allowable stress limit and buckling limit of Slocum respectively.

ii. Titanium Alloy

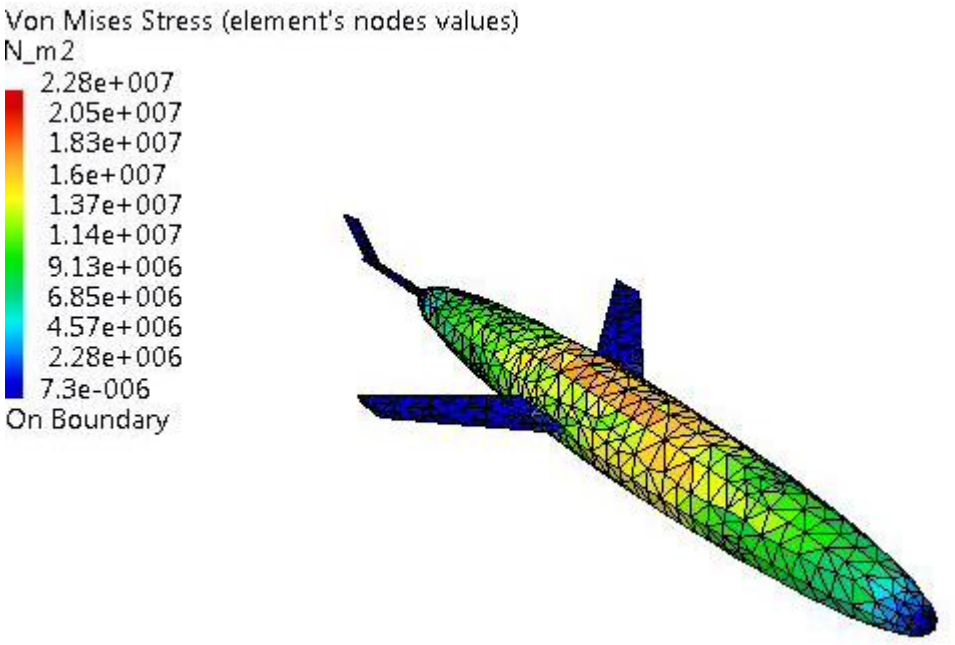

Figure 4.3: Von Mises stress on Slocum with Titanium alloy body

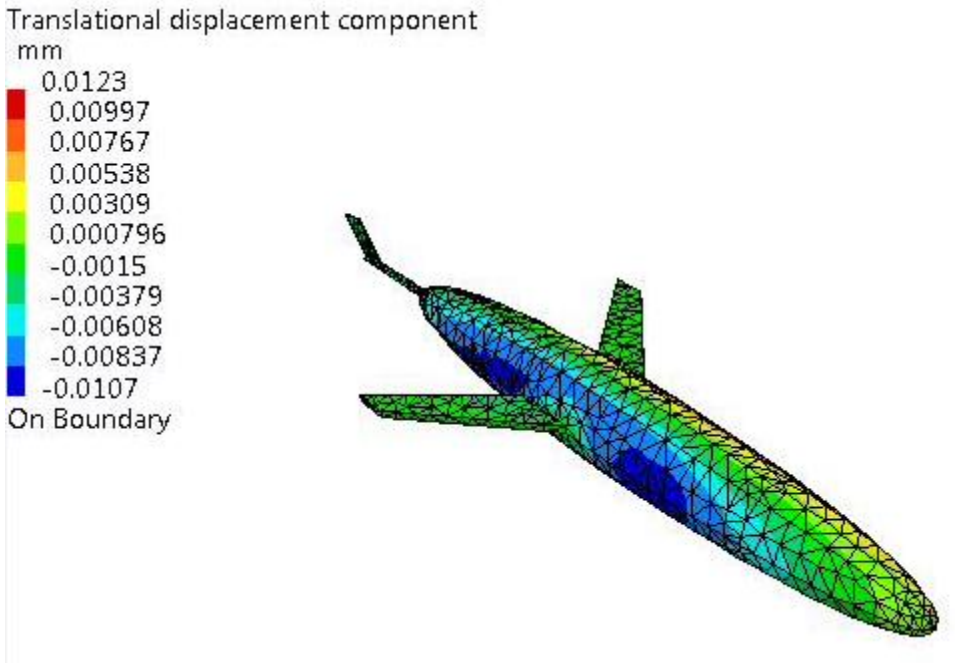

Figure 4.4: Displacement vector on Slocum with Titanium alloy body

Figure 4.3 and Figure 4.4 show Von Mises stress and displacement vector generated on Slocum by numerical method on titanium alloy body respectively. From the analysis above, we can interpret that the most highly distorted element is located at the middle of the glider body which is at 22.8 MPa which is higher than aluminium alloy. On the other hand, the result of translational displacement is highest at the tip and tail of the glider. It is interpreted that the result from the displacement indicated the buckling effect of the glider. Based from the simulation made, both Von Mises stress and translational displacement are within the allowable stress limit and buckling limit of Slocum respectively.

iii. Stainless Steel Alloy

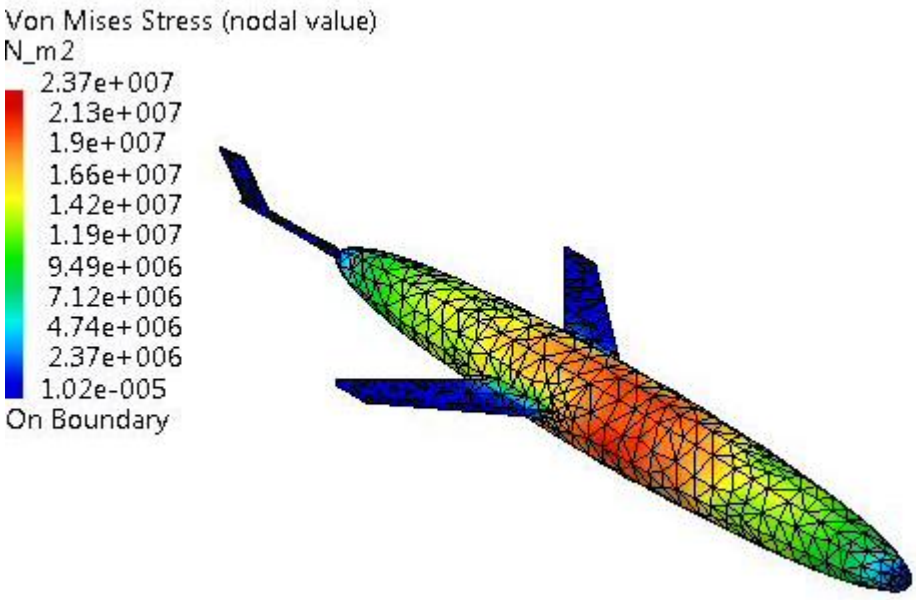

Figure 4.5: Von Mises stress on Slocum with Stainless steel alloy body

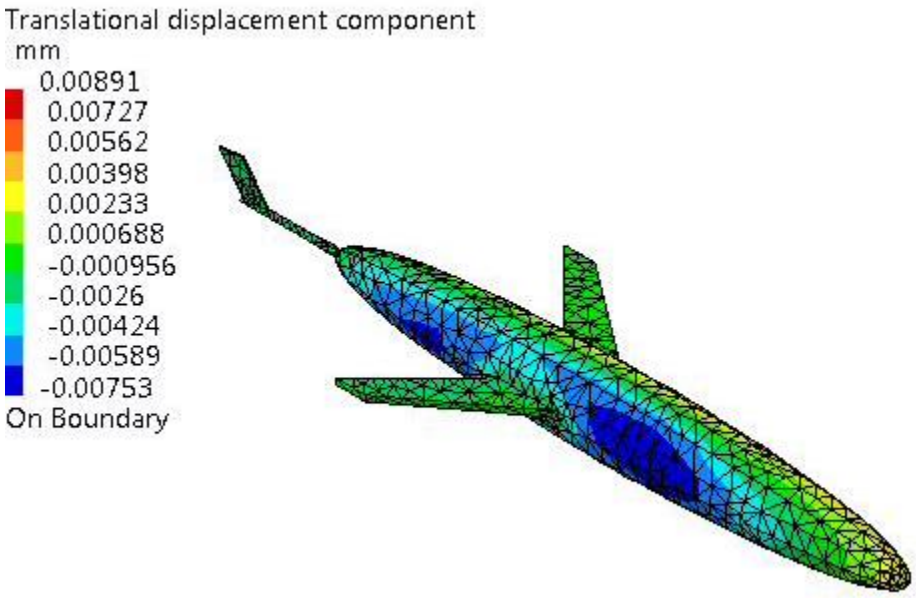

Figure 4.6: Displacement vector on Slocum with Stainless steel body

Figure 4.5 and Figure 4.6 show Von Mises stress and displacement vector generated on Slocum by numerical method on stainless steel alloy body respectively. From the analysis above, we can interpret that the most highly distorted element is located at the middle of the glider body which is at 23.7 MPa which is higher than aluminium alloy but lower than titanium alloy. On the other hand, the result of translational displacement is highest at the tip and tail of the glider. It is interpreted that the result from the displacement indicated the buckling effect of the glider. Based from the simulation made, both Von Mises stress and translational displacement are within the allowable stress limit and buckling limit of Slocum respectively.

SEAGLIDER

i. Aluminium Alloy

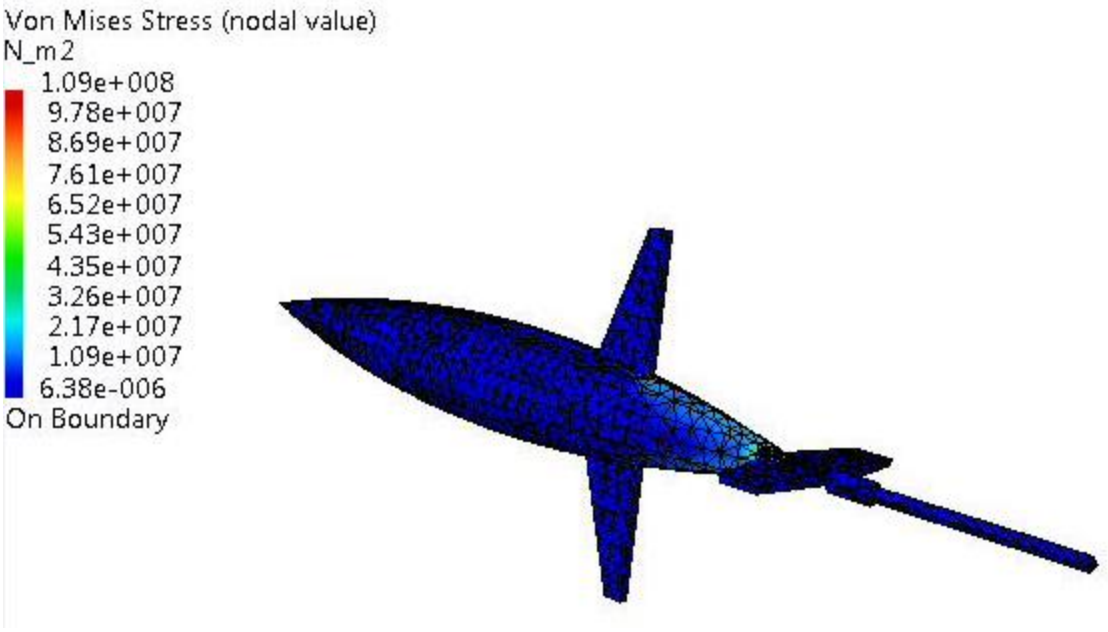

Figure 4.7: Von Mises stress on Seaglider with Aluminium alloy body

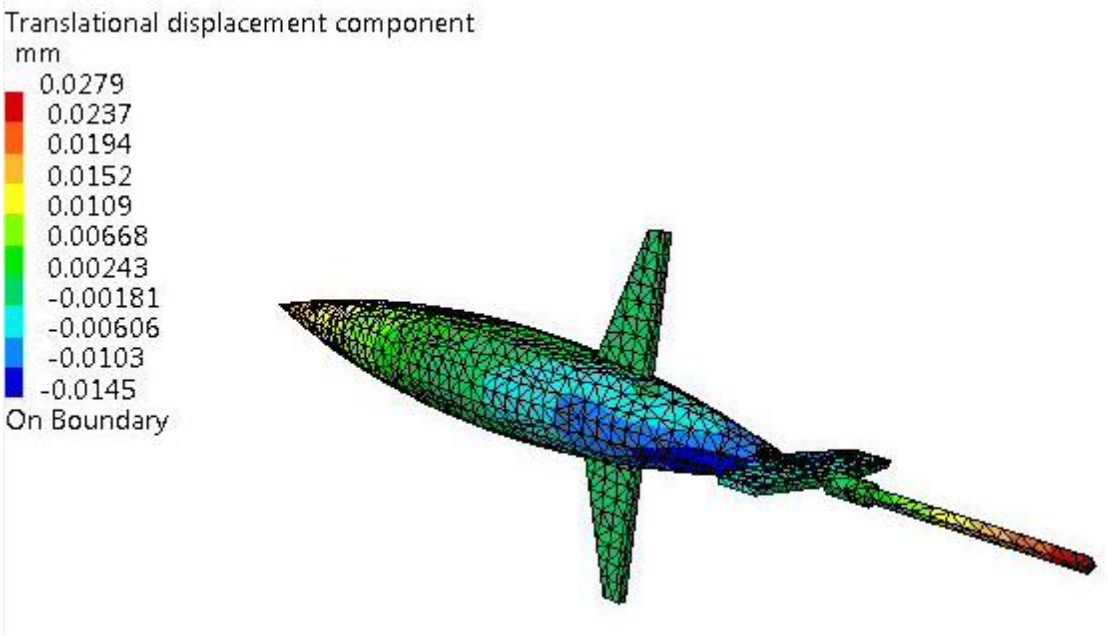

Figure 4.8: Displacement vector on Seaglider with Aluminium alloy body

Figure 4.7 and Figure 4.8 show Von Mises stress and displacement vector generated on Seaglider by numerical method on aluminium alloy body respectively. From the analysis above, we can interpret that the most highly distorted element is located at the middle of the glider body which is at 109 MPa. On the other hand, the result of translational displacement is highest at the tip and tail of the glider. It is interpreted that the result from the displacement indicated the buckling effect of the glider. Based from the simulation made, Von Mises stress of this material has exceeded the allowable yield strength of aluminium alloy which is until 96 MPa.

ii. Titanium Alloy

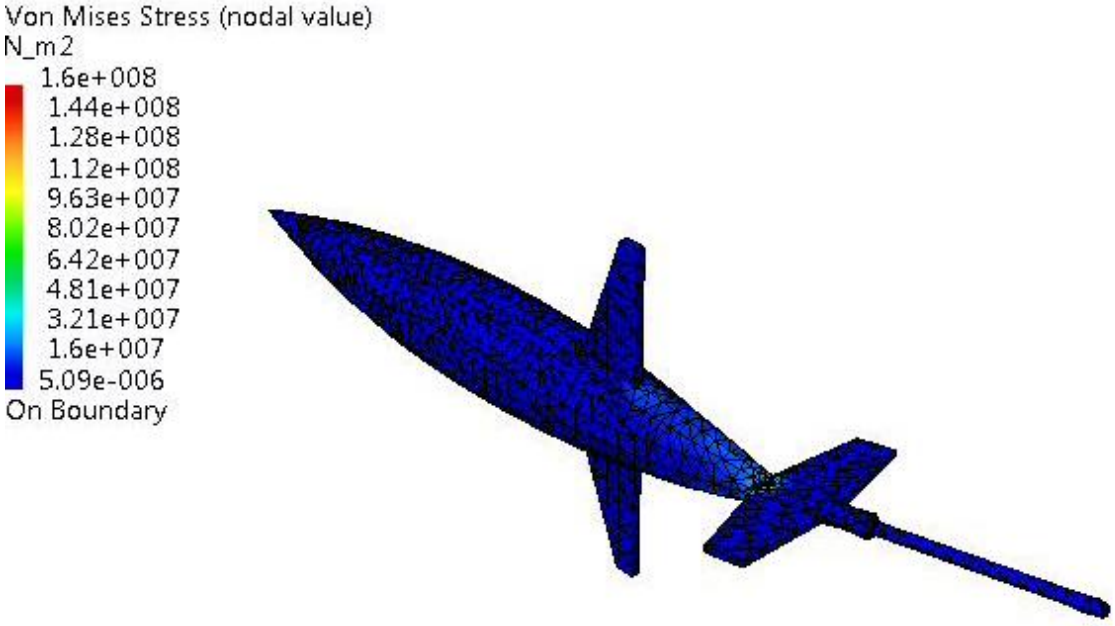

Figure 4.9: Von Mises stress on Seaglider with Titanium alloy body

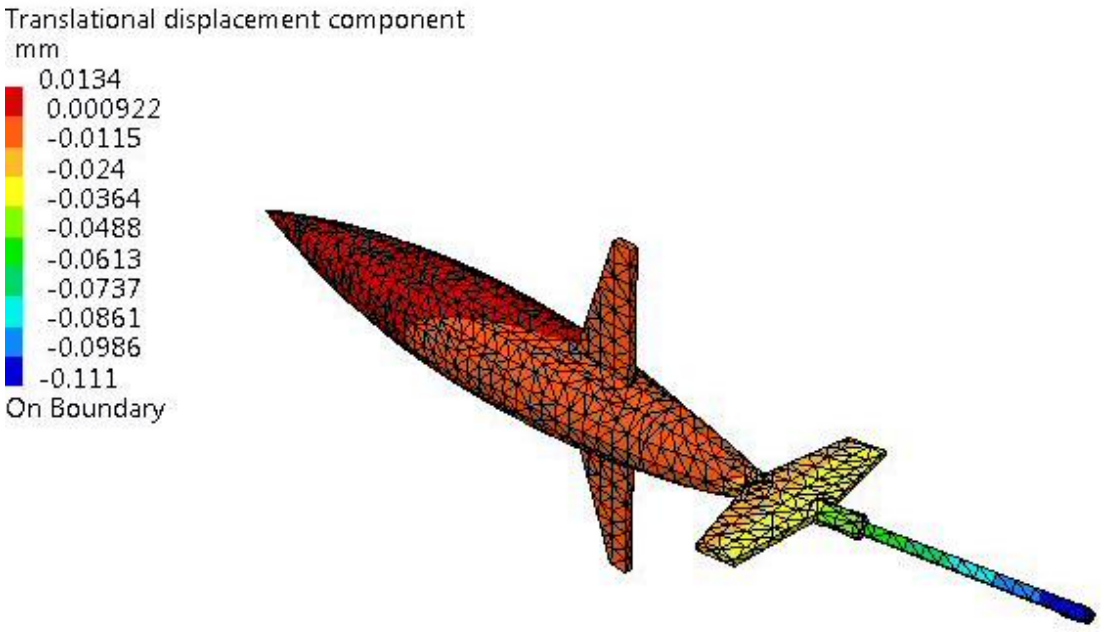

Figure 4.10: Displacement vector on Seaglider with Titanium alloy body

Figure 4.9 and Figure 4.10 show Von Mises stress and displacement vector generated on Seaglider by numerical method on titanium alloy body respectively. From the analysis above, we can interpret that the most highly distorted element is located at the middle of the glider body which is at 160 MPa. On the other hand, the result of translational displacement is highest at the tip and middle body of the glider. It is interpreted that the result from the displacement indicated the buckling effect of the glider. Based from the simulation made, Von Mises stress of this material is still within the allowable stress of titanium alloy.

iii. Stainless Steel Alloy

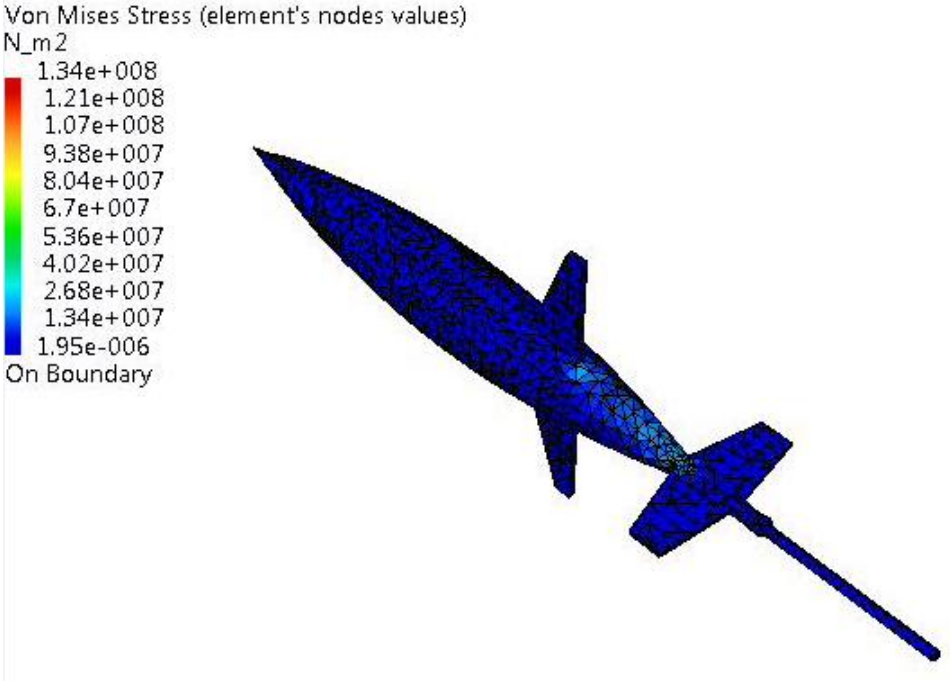

Figure 4.11: Von Mises stress on Seaglider with Stainless steel body

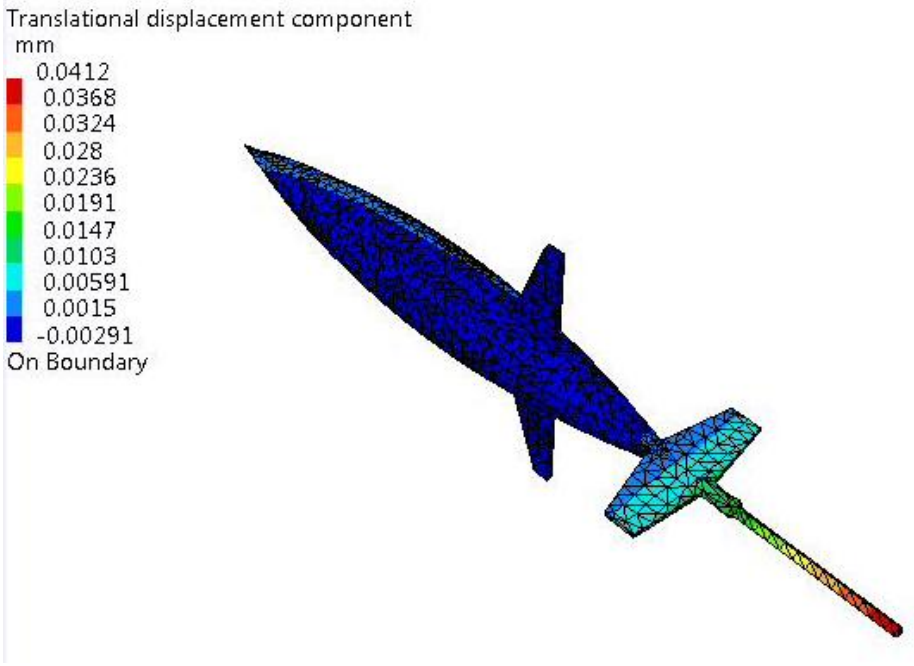

Figure 4.12: Displacement vector on Seaglider with Stainless steel body

Figure 4.11 and Figure 4.12show Von mises stress and displacement vector generated on Seaglider by numerical method on stainless steel alloy body respectively. From the analysis above, we can interpret that the most highly distorted element is located at the middle of the glider body which is at 160 MPa. On the other hand, the result of translational displacement is highest at the tip and middle body of the glider. It is interpreted that the result from the displacement indicated the buckling effect of the glider. Based from the simulation made, Von Mises stress of this material has exceeded the allowable stress of stainless steel.

All values of calculated wall thickness strength check for Slocum are within the permissible values for all three materials used. Even though all three materials are within the allowable stress from the FEA analysis, aluminium alloy is the most suitable material for Slocum body due to its mechanical performance and it is easier to be fabricated among the three materials. The external pressure for Slocum body was designed up to 2.03 MPa. However, only one out of three materials used for Seaglider is within the allowable stress value which is titanium alloy because Seaglider has high operating pressure. Thus, aluminium alloy and stainless steel alloy are not suitable materials for Seaglider hull body design. Table 4.5 and Table 4.6 summarized the results of analytical solution and corresponding to FEA analysis for Slocum and Seaglider respectively. From the simulation, the stress results were analyzed for modification of the design to reinforce the weak regions of the structures.

Table 4.5: Comparison of analytical and numerical solutions for the buckling pressure of Slocum

	Aluminium Alloy			Titanium Alloy			Stainless Steel		
	Analytical	Numerical	Deviation (%)	Analytical	Numerical	Deviation (%)	Analytical	Numerical	Deviation (%)
Displacement (mm)	0.013	0.0151	16.15	0.012	0.0123	2.50	0.01096	0.00891	-18.70
Stress (Mpa)	17.87	18.1	1.29	21.92	22.8	4.01	26.79	23.7	-11.53

Table 4.6: Comparison of analytical and numerical solutions for the buckling pressure of Seaglider

	Aluminium Alloy			Titanium Alloy			Stainless Steel		
	Analytical	Numerical	Deviation (%)	Analytical	Numerical	Deviation (%)	Analytical	Numerical	Deviation (%)
Displacement (mm)	0.028	0.0279	-0.36	0.021	0.0134	-36.19	0.01547	0.0412	-62.45
Stress (Mpa)	97.6	109	11.68	119.75	160	33.61	146.39	134	-8.46

4.2 Hydrodynamic Analysis

4.2.1. Lift and Drag force distribution

For this section, application of momentum conservation of law of an airfoil is adopted for AUG lift and drag force distribution. For this analysis, the distributed forces are due to two sources:

1. Pressure distribution on the AUG body surface
2. Shear stress distribution over AUG body surface

In terms of pressure, the forces act normal to the surface of an AUG body where as shear stress produces tangential force to the surface of the AUG. Due to the integration between these two factors, forces and moments are resulted over the surface of the AUG body profile. Moreover, resultant force are further divided into two other components which are normal force (N), exerts perpendicularly to the chord line and the axial force (A), acts parallel to the chord line.

However, in this study, resultant force is split up into two other components, Lift (L) exerts perpendicularly to the AUG flow direction whereas drag (D) acts in the direction of free stream velocity. On the other hand, angle of attack, θ, of an AUG profile is formed in between the thrust force (T) and chord line of the AUG flow direction.

The equations below are used to estimate the lift and drag forces (L and D) respectively.

$$L = \frac{1}{2}\rho V^2 A C_L \quad (4.4)$$

$$D = \frac{1}{2}\rho V^2 A C_D \quad (4.5)$$

Where;

$\rho = density$

$A = Area\ reference\ chosen\ for\ calculating\ lift\ and\ drag$

$C_L = Lift\ coefficient$

$C_D = Drag\ coeeficient$

$V = Velocity\ of\ fluid$

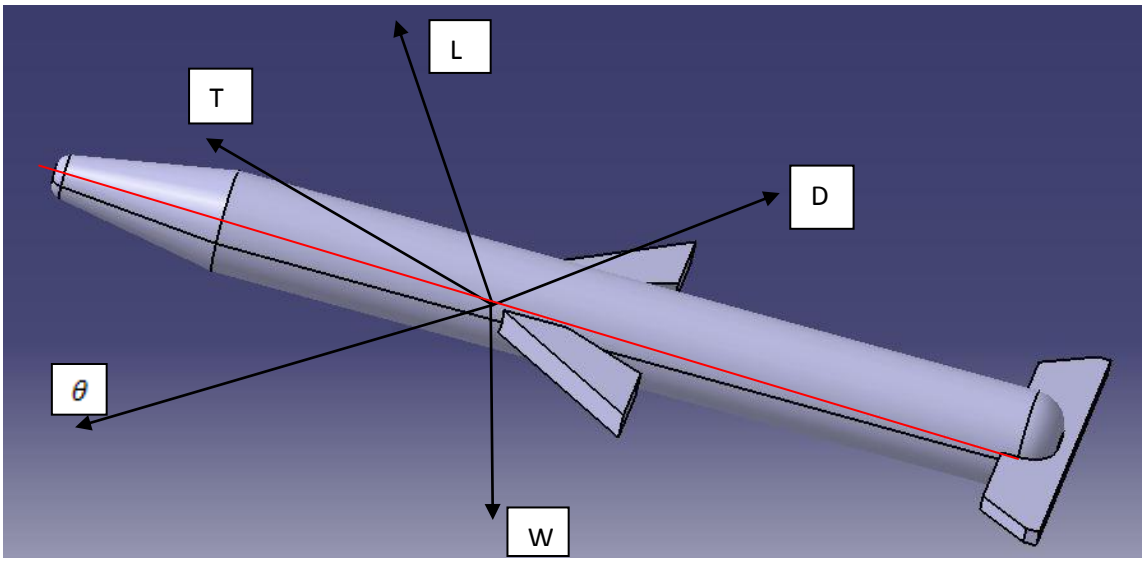

Figure 4.13: Forces distribution acted on a typical AUG CATIA model

4.2.2 Governing Equations

To investigate hydrodynamic study, governing equation is needed in order to analyse hydrodynamic behaviour of the existing AUGs designs. The low speed model analysis will be made in the next project phase at different Reynolds number and angles of attack. The Spatlart Almaras Turbulence equation and continuity equation is chosen due to flow is considered as three dimensional steady state and incompressible.

Continuity equation: [8]

$$\frac{\partial v}{\partial xj} = 0 \quad (4.6)$$

Spatlart Almarass equation: [9]

$$\frac{\partial v}{\partial t} + u_j \frac{\partial v}{\partial x_j} = C_{b1}(1 - f_{t2})Sv + \frac{1}{\sigma}\{[(v - V)V] + C_{b2}|v|^2\} - \left[C_{w1} f_w - \frac{C_{b1}}{k^2} f_{t2} \right] \left(\frac{V}{d}\right)^2 + f_{t1} U^2 \quad (4.4)$$

In case of steady state;

$$\frac{\partial v}{dt} = 0 \quad (4.7)$$

4.2.3 The simulation model

3D simulation model of Slocum and Seaglider were both designed by using CATIA Solid Modelling. Figure 4.13a and Figure 4.13b show the isometric view of Slocum and Seaglider respectively.

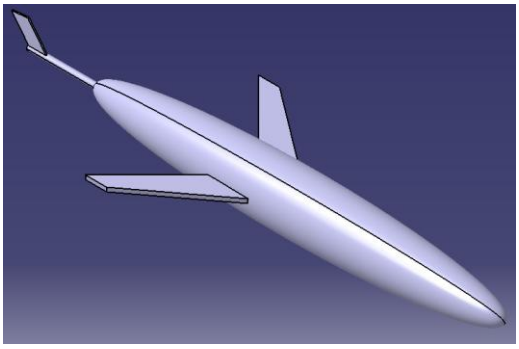

Figure 4.13a: Isometric view of Slocum

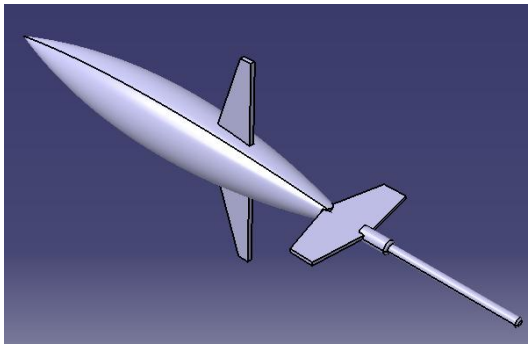

Figure 4.13b: Isometric view of Seaglider

4.2.4 Calculation model by using CFD analysis

For numerical investigation, CFD Ansys Fluent is to be used to verify the analytical values of lift and drag coefficients. Calculation domain is usually formed by

constructing virtual body and RANS equations within the domain are solved. Therefore, a boundary condition is needed to be given for spatial domain.

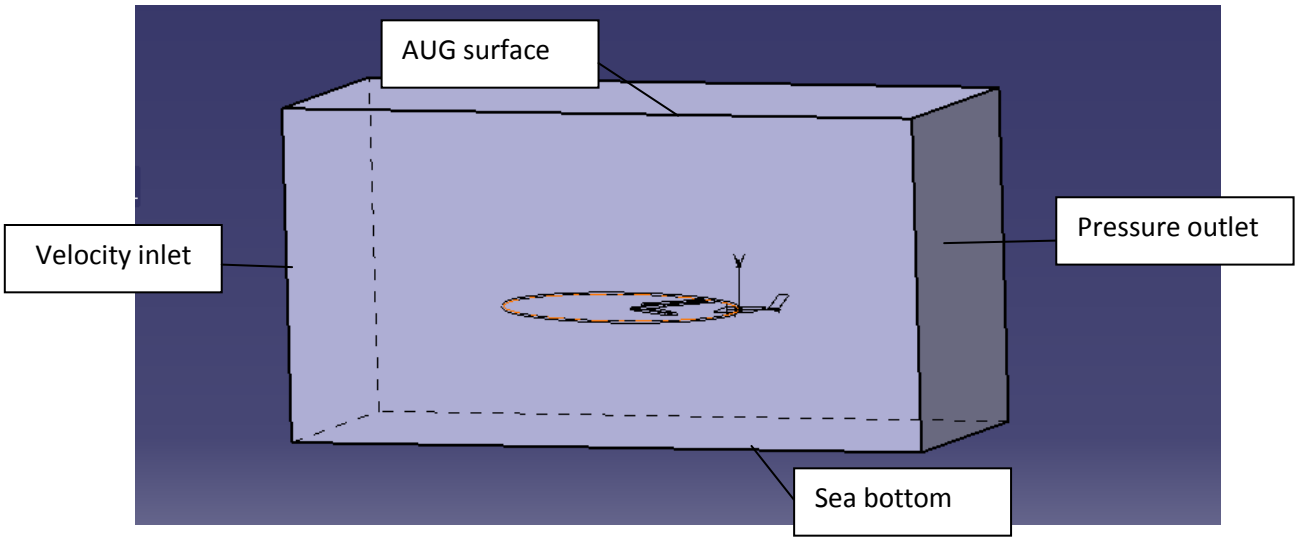

Figure 4.14: Calculation model of AUG moving close to sea bottom by using CATIA

4.2.5 Meshing and boundary conditions

The size function and tetrahedron meshing method was applied on both AUGs to keep the meshes distributing reasonably and to avoid meshing quality problems, maximum cell skewness must not exceed 0.98. The examples of meshing made are shown in Figure 4.15 and Figure 4.16.

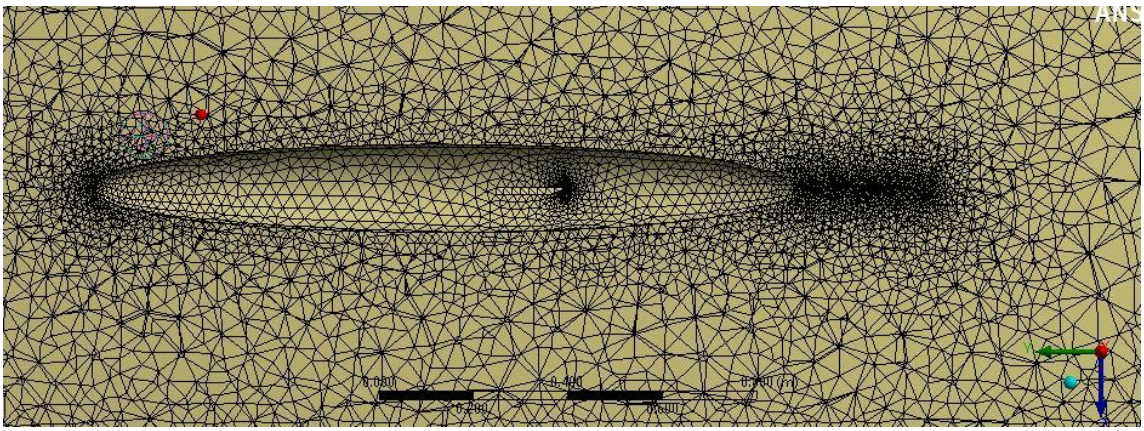

Figure 4.15: Two-dimension rudder mesh of Slocum

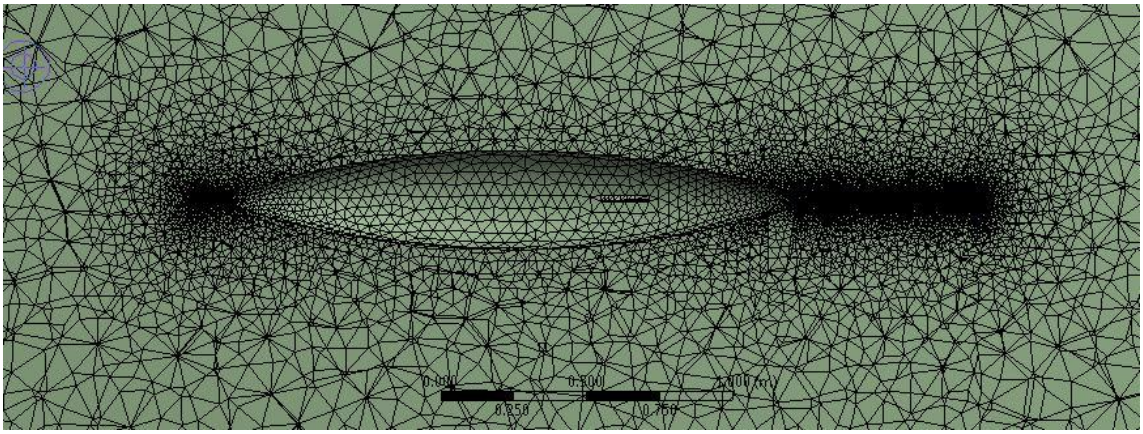

Figure 4.16: Two dimension rudder mesh of Seaglider

Boundary conditions;

1. At inlet boundary condition, 0.4 m/s is set in front of the domain wall with the distance of 5 times larger than the AUGs.
2. At outlet boundary condition, the end of the domain wall is distanced to be 5 times larger than the AUGs.
3. Wall boundary condition; applied non slip condition that the fluid will have zero velocity relative to the boundary.

4.2.6 Analysis of Hydrodynamic Performance

i. Lift vs. Drag

CFD fluent is chosen to simulate and analyse the hydrodynamic performance of Slocum and Seaglider. Lift and drag coefficients are calculated by using different AUGs models. Both AUGs are compared and analyse in further details. For this model analysis, k-epsilon models have been used as the turbulence model. For models with small pressure gradient, k-epsilon model is suitable for free shear layer flows. Besides that, this method is as useful for well-bounded and internal flows where pressure gradients are small.

Lift and drag forces on both AUGs are compared in Figure 4.17. From this analysis, lift force is created by the main wings and AUG body. As the fluid passes the main wings and body, the fluid will be deflected and the direction of the flowing fluid follows the curved body and wings of AUG. Based from Figure 4.17, Seaglider has bigger lift compared to Slocum when drag coefficients are less than 1. However the lift of Slocum model increases gradually and higher than Seaglider when the drag coefficients are more than 1. Due to higher drag generated by the AUGs, glide angles should be taken into consideration by variable buoyancy as shown in the equation below;

$$D = B \sin\theta \quad (4.8)$$

Where;

D = Drag of AUG

B = Net buoyancy

θ = Glide angle

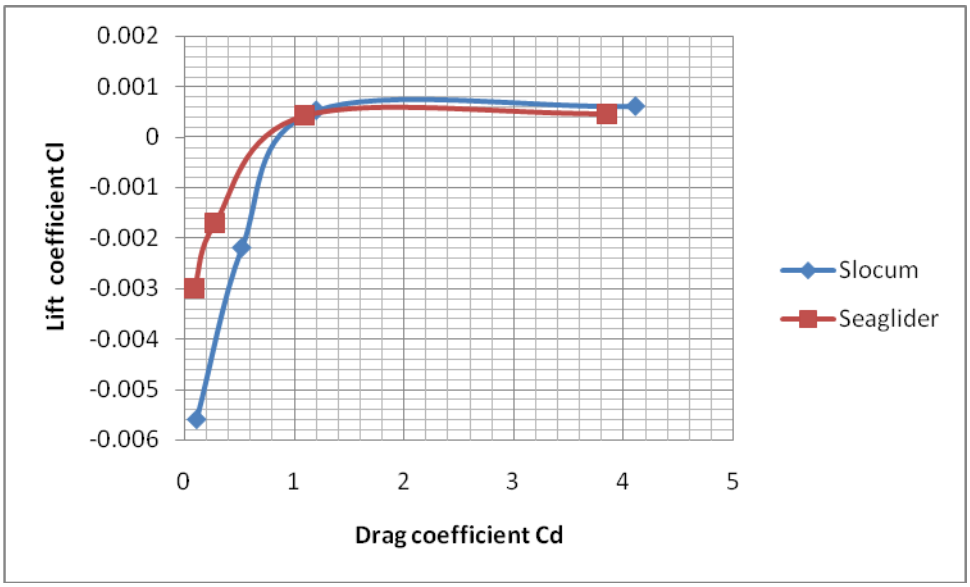

Figure 4.17: Comparison of drag coefficients vs. lift coefficients of Slocum and Seaglider

ii. Effects of Angle of Attack (AoA) on lift and drag coefficients

Figure 4.18 and Figure 4.19 show the relationship of angle of attacks and lift and drag coefficients respectively. The coefficient of lift for both AUGs increased as the AoA increased from -15° to 15°. The AoA increased gradually due to the low cruising speed of both AUGs which was set at 0.4 m/s. On the other hand, both Slocum and Seaglider drag coefficients range from 0.08 to 4.4. Drag coefficients for both model increased as AoA increased. Based from Figure 4.19, drag coefficients for both AUGs are the highest at AoA = 15° compared with other AoA. This phenomenon occurred due to wake formed at the wings of AUGs.

Lift coefficient variations are small compared to drag coefficients. This small variation is because the relative velocity of both AUGs is simulated less than 1 m/s. From the AoA vs lift coefficient graph, it is shown that Seaglider generated higher lift coefficients compared to Slocum until AoA = 5°. However, in Figure 4.19, Seaglider has lower drag coefficients compared to Slocum. Due to different shape of Slocum and Seaglider, lift and drag coefficients are generated slightly different. Seaglider model has thinner shape and has geometry which is more closely to NACA foil compared to Slocum model. The NACA foil is widely used for underwater vehicles rudders which produce higher lift and lower drag. Form the hydrodynamic perspective, Seaglider has better hydrodynamic performance compared to Slocum due to its higher lift and lower drag.

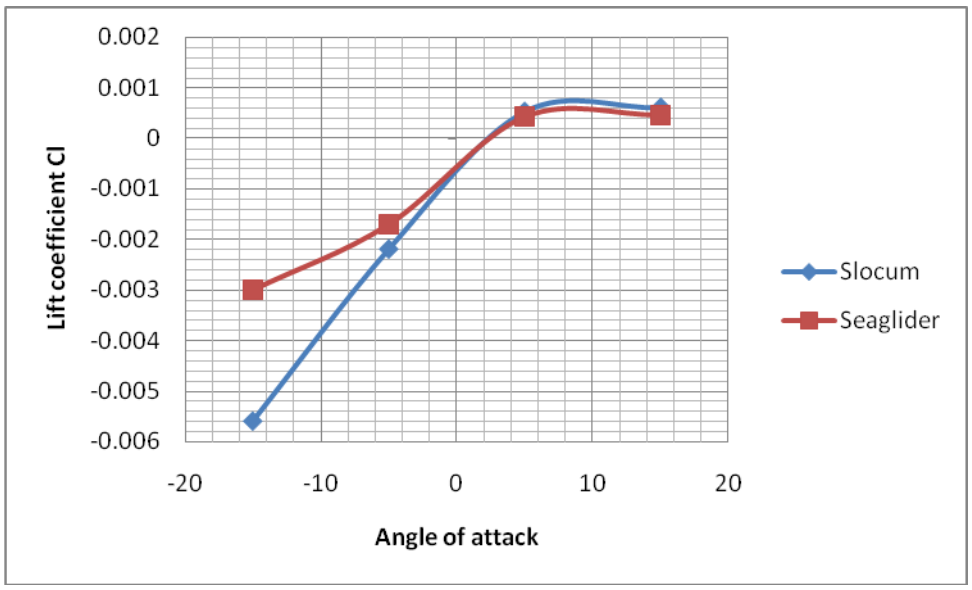

Figure 4.18: Effect of angle of attacks on lift coefficients

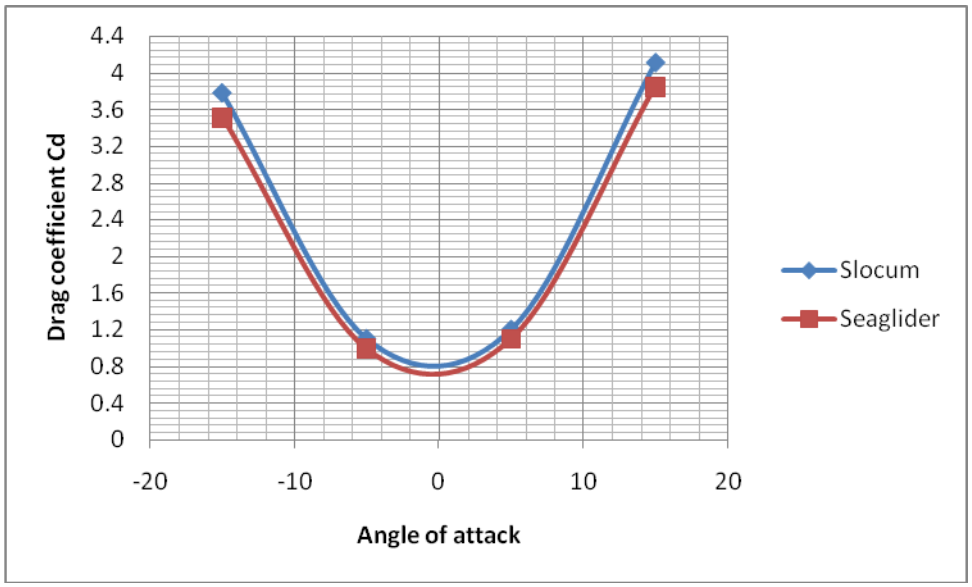

Figure 4.19: Effects of angle of attacks on drag coefficients

L/D ratio is the amount of lift created by the AUGs wings, divided by the drag force generated by flowing fluid. In this finding, higher L/D ratio is preferred because lift with lower drag leads to better glide performance and glide ratio. Based from Figure 4.20, Seaglider has maximal lift to drag ratio compared to Slocum. The position of the main wings influenced the L/D and it has little effect on AUGs

gliding efficiency. The best and maximum L/D ratio for Seaglider occurs when AoA = 8°. Similarly, Slocum has the highest L/D ratio when AoA = 8°. However, since Seaglider generated slightly higher L/D ratio compared to Slocum, Seaglider has better hydrodynamic wing design than Slocum. Thus, the bigger ratio corresponds to higher gliding efficiency.

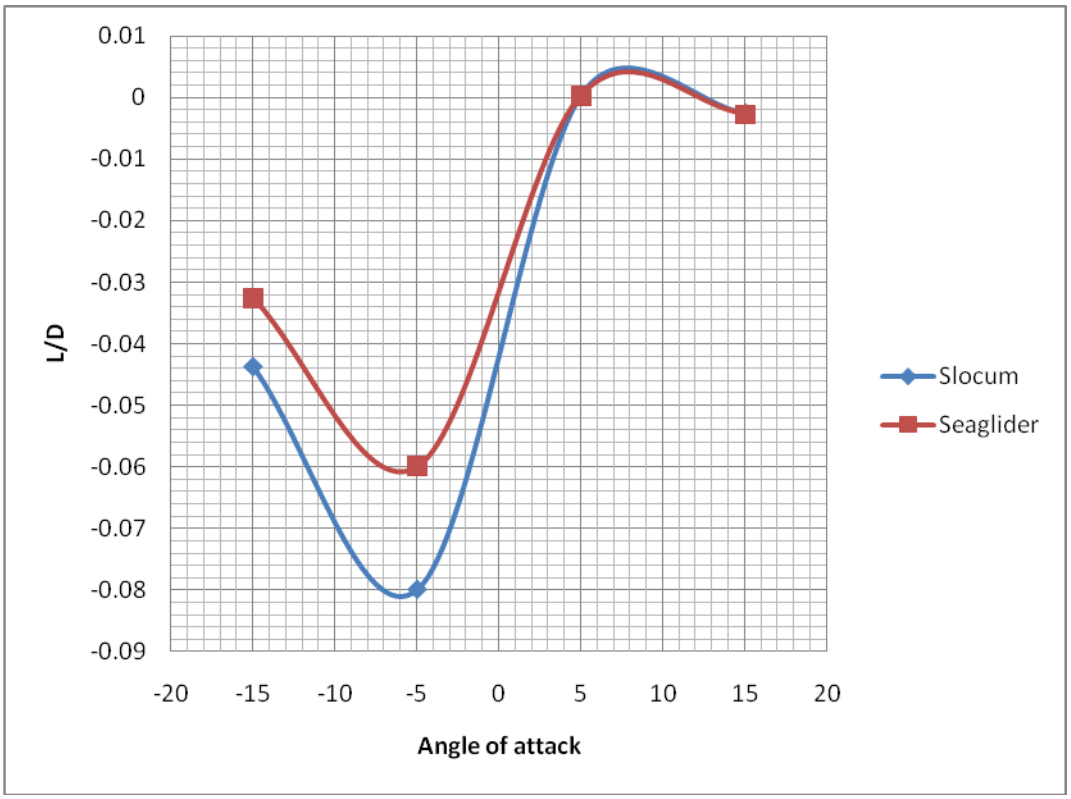

Figure 4.20: Relationship of AoA and lift drag ratio of Slocum and Seaglider

iii. Stream lines

At AoA = 15°, it is found that drag forces are at maximum for both AUGs. Therefore, wake is formed at the upper surface of the AUGs. From Figure 4.21, it is shown that Seaglider has maximum velocity of 0.537 m/s.

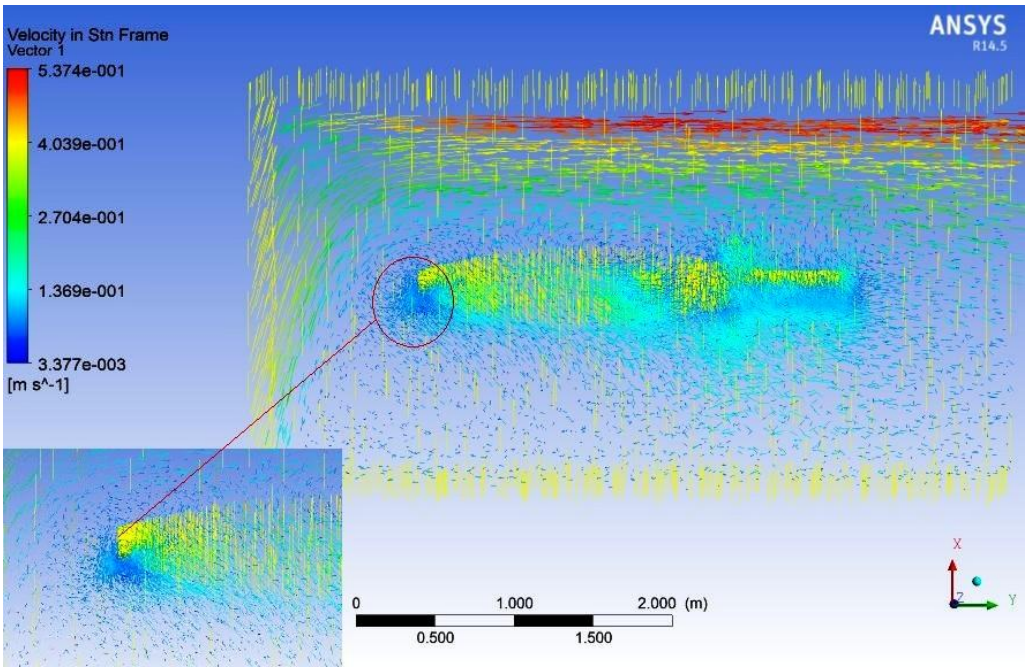

Figure 4.21: Streamline at AoA = 15° on Seaglider

iv. Velocity profiles

Figure 4.22 and Figure 4.23 show the velocity profiles of Slocum and Seaglider at AoA = 15° respectively. Magnitude of velocity changes as the fluid flows along the AUG surface. Based from both figures, velocity is at its minimum at the area around the nose of both AUGs since this surface exerts highest pressure magnitude. Furthermore, fluid velocity increases as the fluid flows along the curved surface of the tip of the gliders. Thus, higher velocity is formed at the upper surface of the glider. However, as AoA increases, it is found that the flow along the upper surface of AUGs decreases. Therefore, at AoA= 15°, low velocity if formed at the upper surface in both Figure 4.23 and Figure 4.22. As mentioned in previous section, wake is formed at the upper surface of AUGs due to gliders' low cruising speed at 0.4 m/s. Wake region continues to develop as the AoA increases.

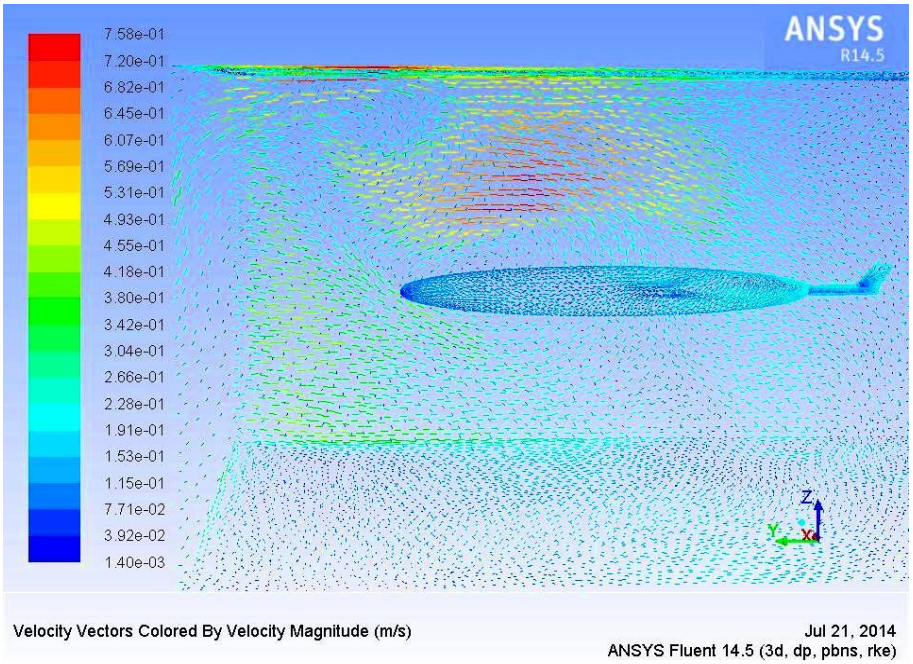

Figure 4.22: Velocity profile of Slocum at AoA = 15°

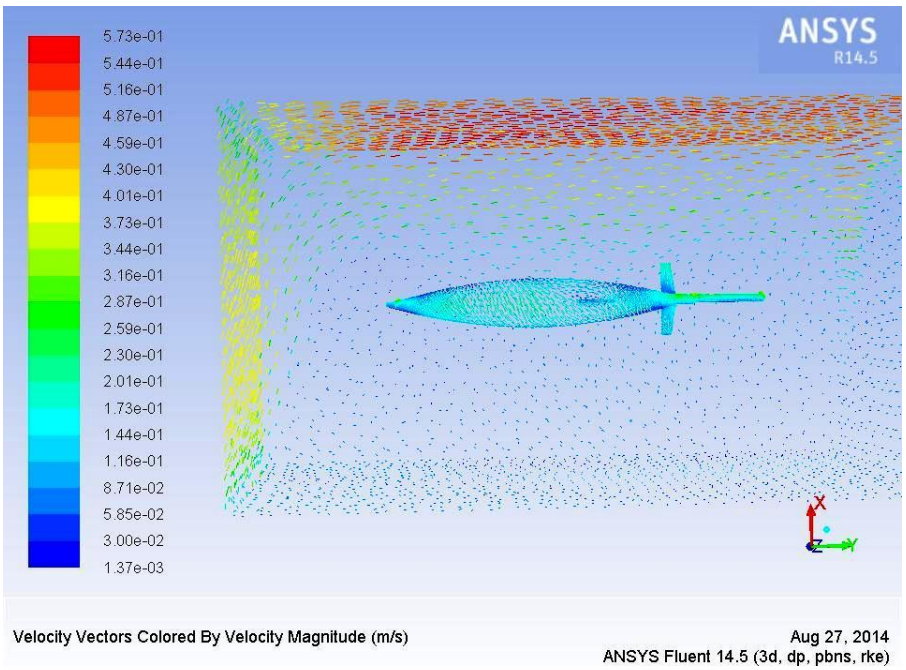

Figure 4.23: Velocity profile of Seaglider at AoA= 15°

v. Pressure distribution

Figure 4.24 and Figure 4.25 show the pressure distributions on Slocum and Seaglider at speed of 0.4 m/s respectively when AoA = 0°. Generally, there is an inclination that pressure on AUGs is at highest from the inlet side. Thus,

high pressure region exerts at the head of AUGs while low pressure region exerts at the tail which created the pressure drag on the AUGs. However, since the AUGs are specified to have constant velocity at 0.4 m/s, we can interpret that pressure are equally distributed on the AUGs body as shown in Figure 4.24 and Figure 4.25

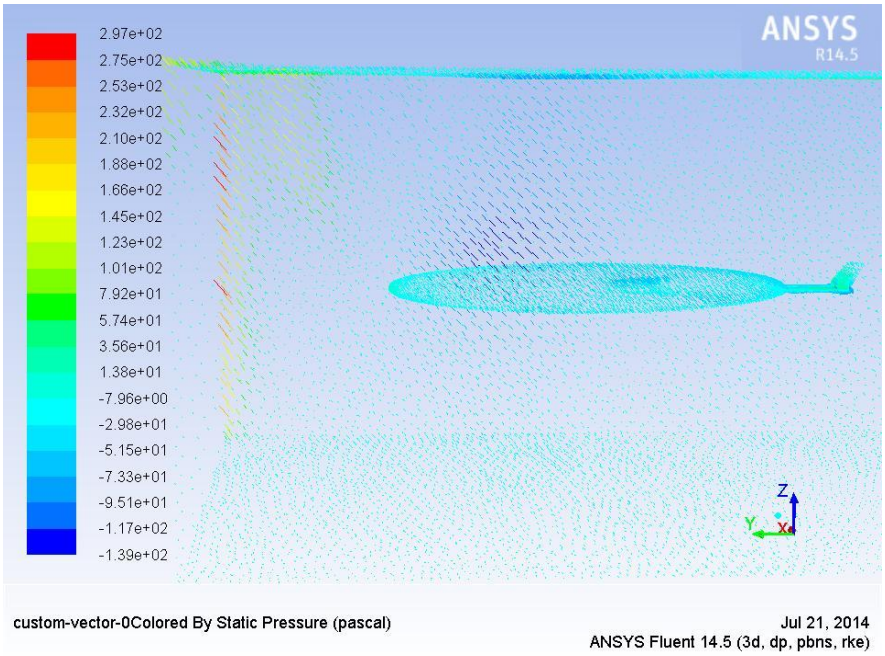

Figure 4.24: Pressure distribution on Slocum at AoA= 0°

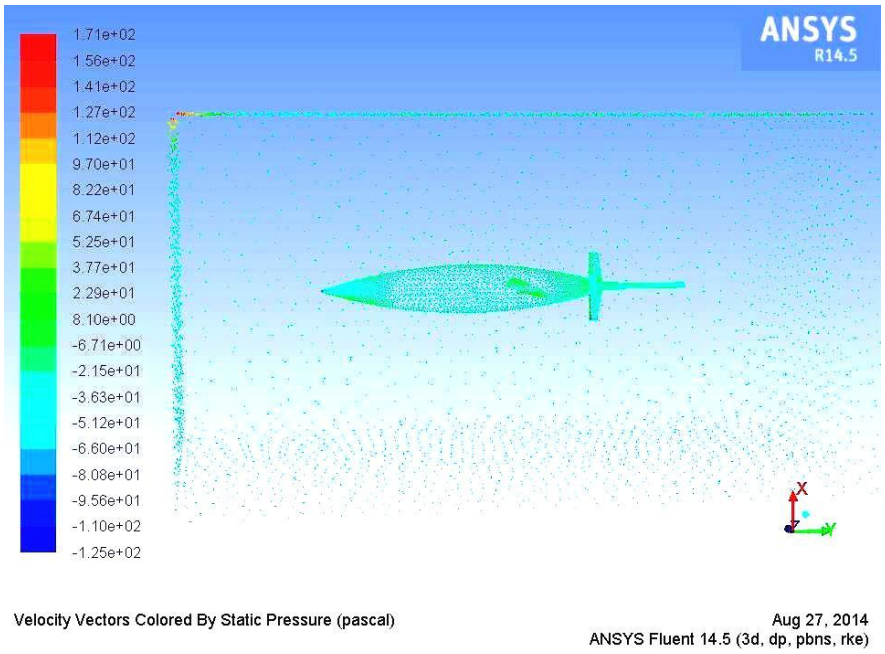

Figure 4.25: Pressure distribution on Seaglider at AoA= 0°

CHAPTER 5
CONCLUSION

This study focuses on comparative of structural design and hydrodynamic performance of the existing gliders, Slocum and Seaglider which have different operating pressure and geometry. The FEA analysis effects on the structural of the material tested on Slocum and Seaglider which are Aluminium alloy, Titanium Alloy and Stainless Steel Alloy. On the other hand, CFD analysis shows hydrodynamic effects on the AUGs especially in the glide mode.

For structural analysis, it is found that aluminium alloy is the most suitable material for Slocum and gliders which work similarly to Slocum's operating pressure and depth. Even though all three materials are within their allowable stress, aluminium alloy is chosen due to its mechanical performance and ease of fabrication. However, only one out of three materials used for Seaglider is within the allowable stress value which is titanium alloy because Seaglider has high operating pressure. Thus, aluminium alloy and stainless steel alloy are not suitable materials for Seaglider hull body design.

For hydrodynamic analysis, it is found that location of the AUGs wings have great impact the glide stability but has less impact on glide efficiency. From the analysis made, Seaglider has higher lift and lesser drag than Slocum. Seaglider model has thinner shape and has geometry which is more closely to NACA foil compared to Slocum model. The NACA foil is widely used for underwater vehicles rudders which produce higher lift and lower drag. Form the hydrodynamic perspective, Seaglider has better hydrodynamic performance compared to Slocum due to its higher lift and lower drag. It was found that for both gliders, wake is formed when AoA = 15° because drag force is at maximum.

REFERENCES

[1] Henry Stommel. The Slocum Mission. *Oceanography*, 2:22–25, 1989.

[2] A. Bender, D. M. Steinberg, A. L. Friedman, S. B. Williams. "Analysis of Autonomous Underwater Glider", Australian Center for Field Robotics, University of Sydney, 2006.

[3] Joshua G. Graver and Naomi Ehrich Leonard. Underwater glider dynamics and control. In 12th International Symposium on Unmanned Untethered Submersible Technology, Durham, NH, USA, August 2001.

[4] J. Sherman, R. E. Davis, W. B. Owens, and J. Valdes. The autonomous underwater glider "Spray". IEEE Journal of Oceanic Engineering, 26(4):437–446, October 2001.

[5] C. C. Eriksen, T. J. Osse, R. D. Light, T. Wen, T. W. Lehman, P. L. Sabin, J. W. Ballard, and A. M. Chiodi, "Seaglider: A long-range autonomous underwater vehicle for oceanographic research," IEEE J. Oceanic Eng., vol. 26, pp. 424–436, Oct. 2001.

[6] Davis, R. E., C. C. Eriksen and C. P. Jones. 2003. Autonomous buoyancy-driven underwater gliders. In: Technology and Applications of Autonomous Underwater Vehicles, ed. G. Griffiths, pp. 37-58. Taylor and Francis.

[7] P. Simonetti, "SLOCUM Glider Design," Webb Research Corp., Falmouth, MA, Rep. Webb Research Corp.,
1992.

[8] Ting M.C., M. Abdul Mujeebu, M.Z. Abdullah and M. R. Arshad, 2010. Study on hydrodynamic performance of shallow underwater glider platform. USM,Nibong Tebal,Penang.

[9] M. Zheng, Z. Hua, Z. Nan and M.D. Mei. "Study on Energy and Hydrodynamic Performance of Underwater Glider", Journal of Ship Mechanics, vol.10, pp. 53-60, June,2006